www.s2is.org
International Journal on Smart Sensing and Intelligent Systems
ISSN 1178-5608

EFFECTS OF PLACEMENT ERRORS ON PERFORMANCE OF VLF METAL DETECTOR HEADS

Lawrence J. Carter
Department of Electrical & Computer Engineering
University of Auckland
Auckland, New Zealand
Email: lj.carter@auckland.ac.nz

Zhuoran Tang
Department of Electrical & Computer Engineering
University of Auckland
Auckland, New Zealand
Email: ztan024@aucklanduni.ac.nz

Submitted: Nov. 11, 2011 ***Accepted: Nov. 30, 2011*** ***Published: Dec. 3, 2011***

Abstract- Metal-detector performance depends heavily on the sensor head. Errors in coil placement within the head can lead to degradation in detector performance. Electromagnetic modelling of typical very-low-frequency detector heads shows the effect of coil placement errors on detector sensitivity. Provided the bucking coil 'tracks' the receive coil, required error corrections can remain small. A correctly-aligned head could detect a gold ring target at a range of about 12 cm.

Index terms: metal detector; sensor head modelling; metal detector sensitivity

I. INTRODUCTION

Early metal detectors (MDs) were developed at the end of the 19th century. Alexander Graham Bell is credited with the invention of the first MD in 1881 [1]. Technology improved during the world wars of the 20th century when it became apparent that MDs could be used to find buried landmines [2,3]. Research has continued to improve technology for landmine and tripwire detection [12-18]. Today MDs are used in a wide range of applications from military to hobbyist [3].

Figure 1: Handheld metal detector [9]

II. METAL DETECTORS

A number of different detector technologies exist, including pulse-induction (PI) and very-low frequency (VLF). Both technologies depend on the sensing of eddy currents induced by the MD into a metallic target. The process is based on Faraday's law of induction. Output voltage V of a sensing coil is given by:

$$V = -n \cdot \frac{\mathrm{d}\Phi}{\mathrm{d}t} = -n \cdot A \cdot \frac{\mathrm{d}B}{\mathrm{d}t} = -\mu_0 \cdot n \cdot A \cdot \frac{\mathrm{d}H}{\mathrm{d}t} \qquad (1)$$

where Φ is the magnetic flux passing through a coil with an area A and a number of turns n. Tumanski (2007) gives a useful review of coil-based sensors [4]. Yamazaki, Nakane, and Tanaka (2002) cover basic MD theory [5].

The PI MD typically uses a single coil for both transmit and receive functions. A pulse of current is passed through the coil, and the subsequent decay of the coil voltage is observed. The presence of a target is indicated by a change in the decay rate, which may be detected by amplifying and integrating the coil voltage waveform [6,7].

VLF MDs typically operate with continuous very low-frequency (3-30 kHz) sine-wave signals. A common configuration is to have three concentric coplanar coils. The outer coil performs the transmit function, and is driven from a sine-wave voltage source. It couples energy into the metallic target, and causes eddy currents to flow in it. The inner coil performs the receive function, and is used to detect the magnetic fields produced by the target eddy currents. A feature of VLF detectors is their ability to make use of phase information in the received signal to discriminate between different kinds of metal target [8]. Figure 1 shows a typical handheld MD [9].

The strong signal in the transmit coil will also couple energy into the receive coil directly, and if this is too large it will mask the small signal from the target. An important feature of VLF MD design is to ensure that the leakage signal V_R is minimised, enabling a high-gain amplifier to be used on the receive coil output to give good detector sensitivity. The third coil in the VLF MD head is a so-called *bucking* coil, and usually surrounds the receive coil and is close to it. The bucking coil is fed with some of the transmit signal and is usually wound in the opposite sense to the transmit coil, so that the transmit field is cancelled in the vicinity of the receive coil [10,11]. The effectiveness of this action can be assessed by measuring the direct-coupled receive coil voltage V_R. Ideally this should be zero.

III. DETECTOR HEAD DESIGN

All common MDs use coils in their sensor heads. Where multiple coils are used, there is scope for placement errors which in turn may affect sensor performance. In the VLF detector, typically three concentric coplanar coils are used, as described above. If there is an error in size or placement of the receive or bucking coils, this will upset the signal cancellation described above, allowing transmit signal to be coupled directly from the transmit coil into the receive coil, thereby swamping the target signal. If the directly-coupled signal V_R can be minimised, this will allow a better signal to interference ratio at the sensor-head output. Hence V_R can be used as a measure of performance: the smaller the value of V_R, in principle the better the MD sensitivity and performance.

In this paper we report on a performance analysis of a VLF MD head, using the electromagnetic modelling software *JMAG*™. The receive coil voltage V_R is used as a performance measure.

IV. ERRORS IN HEAD LAYOUT

Figure 2 shows two scenarios considered, both involving a lateral displacement error x of the receive coil, which however remains coplanar with the transmit coil.

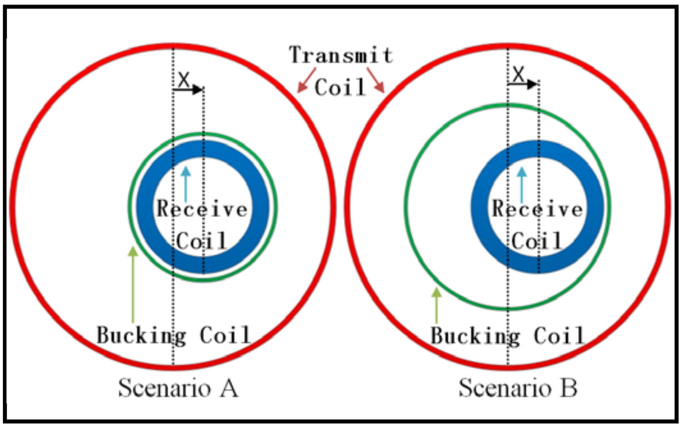

Figure 2: Scenarios A and B for coil displacement

In scenario ‘A’ the bucking coil ‘tracks’ the receive coil and remains concentric with it. In scenario ‘B’ the bucking coil remains concentric with the transmit coil.

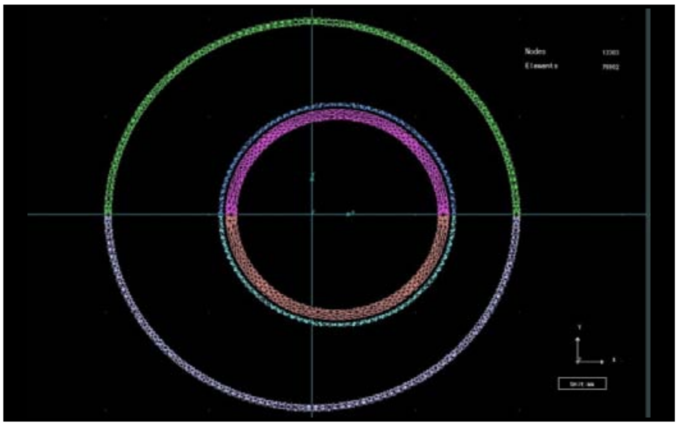

Figure 3: *JMAG*™ mesh for VLF MD modelling

Figure 3 shows the *JMAG*™ mesh used for analysis of scenario 'A'. This was based on an existing VLF MD head design [12]. The transmit coil was provided with a 12 kHz sine-wave input signal of 10 V peak value. For each displacement x of the receive coil, various voltages V_B were supplied to the bucking coil, and the resulting value of leakage voltage V_R obtained.

V. Target Detection

In addition to modelling the effect of coil placement errors in terms of receive coil voltage V_R, it was possible to show the performance of the detector with a metal target. For this purpose a gold ring of diameter 21 mm was used in the model. This was placed centrally below the MD head, and moved away along the z-axis. Values of V_R were plotted against target distance z.

VI. Results

A. *Scenario 'A' (no bucking coil)*

Figure 4 shows results for Scenario 'A', in which first of all the simulation was done with no bucking coil. The receive coil begins at its correct position, concentric and coplanar with the transmit coil. It is then moved laterally a distance x, while remaining coplanar. Receive coil voltage V_R is plotted versus x for displacements up to 30 mm. The leakage voltage increases with displacement, with an increasing slope. This shows explicitly that a placement error of the receive coil will cause loss of sensitivity in the MD.

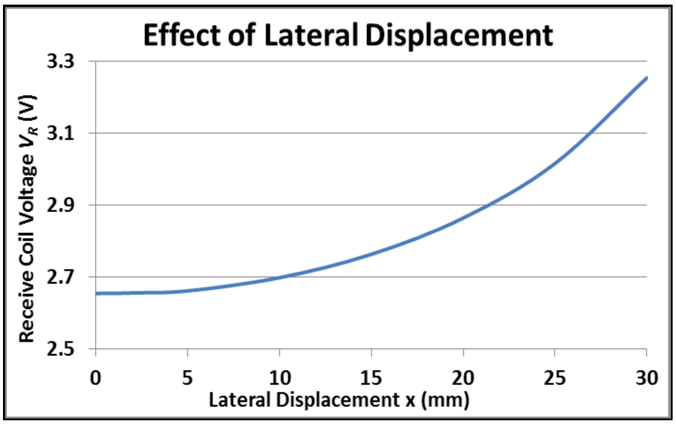

Figure 4: Results for Scenario 'A', no bucking coil

B. Scenario 'A' (with bucking coil)

With the receive coil back in its correct position, the bucking coil was reinstated so that all three coils were concentric and coplanar. With signal on the transmit coil as before, the bucking coil was supplied with a voltage V_B in the range 0 to 0.5 V and the resulting values of V_R were found. The results are shown in Figure 5.

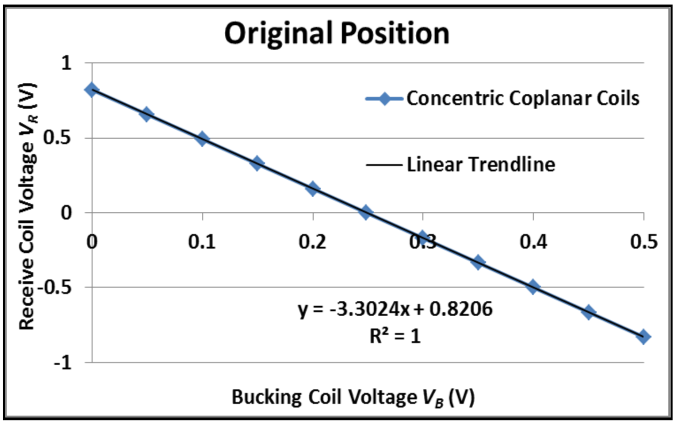

Figure 5: V_R vs V_B for concentric coils

Each of the eleven points in Figure 5 required a complete *JMAG*™ simulation. We can see that it is possible to find a value of V_B for which the leakage voltage V_R is zero, corresponding to maximum sensitivity of the MD. The graph shows that there is a linear relationship between V_R and V_B.

Next, we consider the case in scenario 'A' in which the receive coil is displaced laterally from its central position by various values of *x* between 5 and 30 mm. The bucking coil remains around the receive coil and moves with it, as shown in Figure 6.

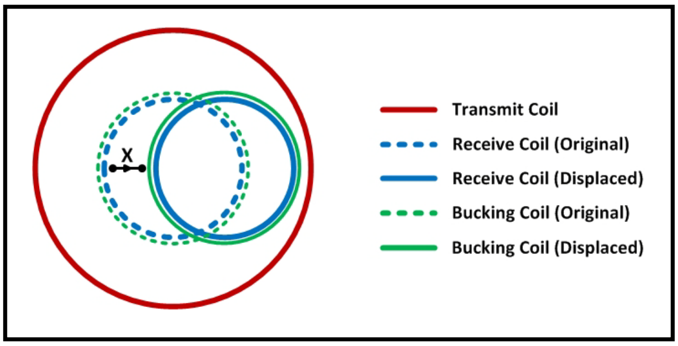

Figure 6: Displacement, receive coil concentric with bucking

For this case, values of V_R vs V_B are shown in Figure 7, plotted for various displacements x in the range 5 to 30 mm. It can be seen that as x increases, the zero-crossing point increases, indicating that a greater bucking voltage is needed to maintain maximum sensitivity. However, the effect is quite small over this range. The curves are linear and have similar gradients.

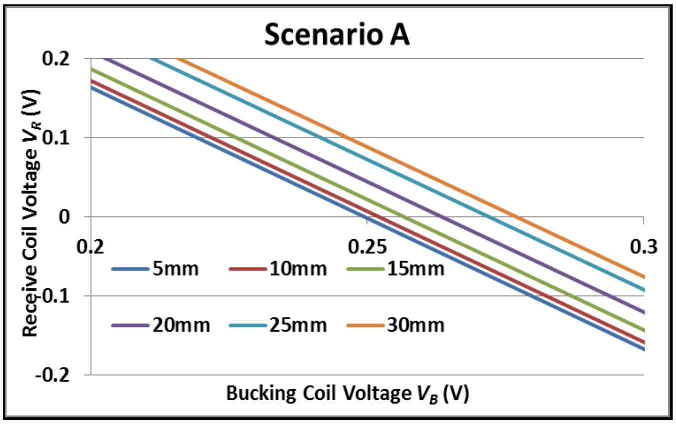

Figure 7: V_R vs V_B for receive coil concentric with bucking

If we define $V_B{}'$ to be the value of bucking voltage to give ideal performance, i.e., $V_R = 0$, then values of $V_B{}'$ can be extracted and plotted versus displacement x as shown in Figure 8.

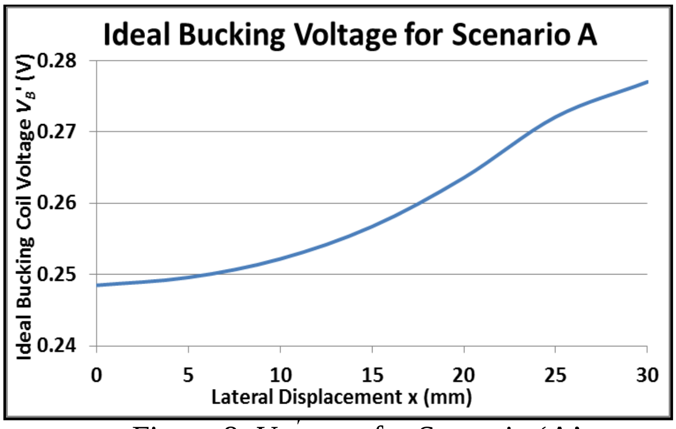

Figure 8: $V_B{}'$ vs x for Scenario 'A'

Figure 8 shows that, provided the bucking coil stays with the receive coil, even quite large displacements do not require much change in bucking coil voltage.

C. *Scenario 'B'*

In scenario 'B', we allow the receive coil to be laterally displaced as before, but this time the bucking coil stays concentric with the transmit coil. This is illustrated in Figure 9.

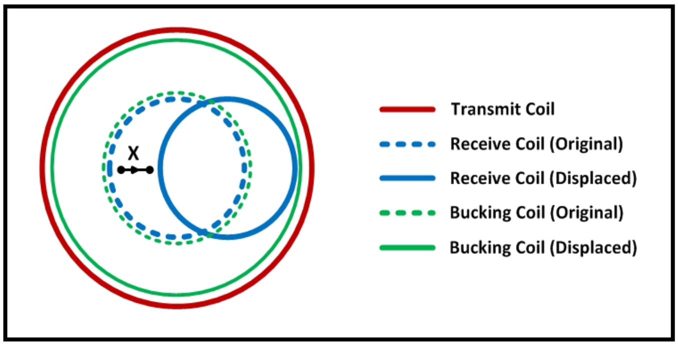

Figure 9: Displacement, bucking coil concentric with transmit

In this case, the bucking coil increases in diameter as the receive coil moves. To be able to compare results, the inductance and total volume of the bucking coil are kept constant, which means that the number of turns reduces as the coil gets bigger. The minimum separation between receive and bucking coils is maintained constant.

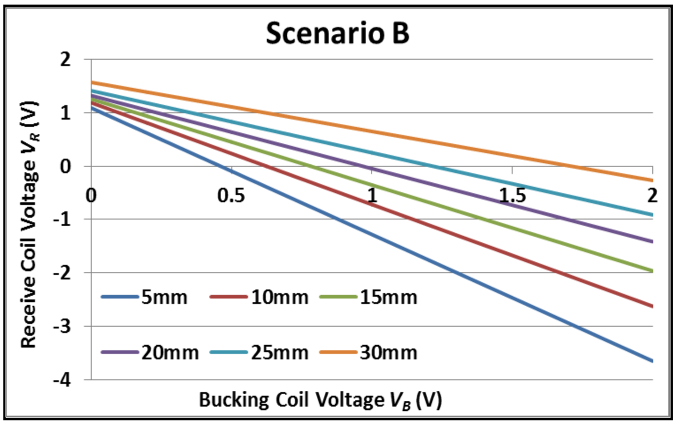

Figure 10: V_R vs V_B for bucking coil concentric with transmit

Figure 10 shows a plot of V_R versus V_B for scenario 'B', using the same displacement values *x*. As before, the zero-crossing point increases with *x*, indicating that a greater bucking voltage is required; however correction is still possible in each of the cases considered. The curves remain linear, but now the gradients change with *x*.

Figure 11 shows how the ideal bucking voltage $V_B{}'$ varies with displacement in scenario 'B'. It can be seen that over the same displacement range, the variation in $V_B{}'$ is much greater than before (compare with Fig. 8).

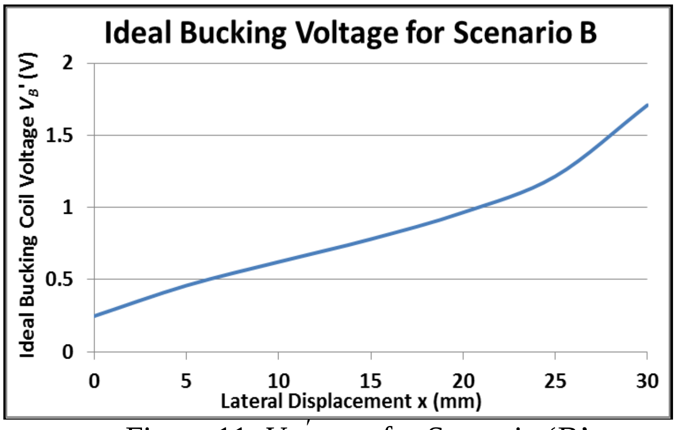

Figure 11: $V_B{}'$ vs x for Scenario 'B'

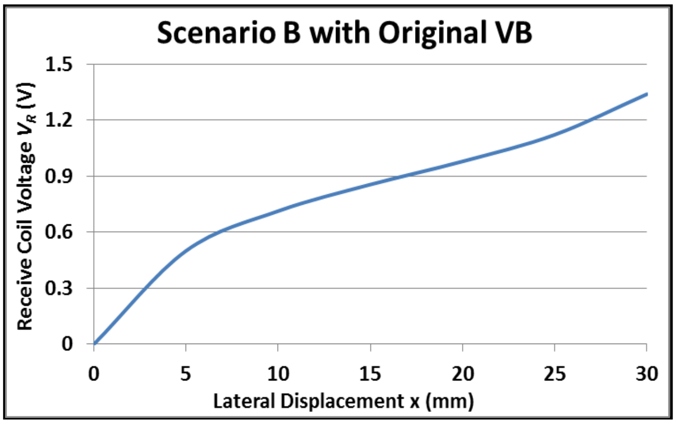

Figure 12: V_R vs x for Scenario 'B', V_B constant

Figure 12 shows how leakage voltage V_R varies with displacement in scenario 'B', if V_B is not corrected for displacement but remains at its zero-displacement value.

D. Performance with target

Figure 13 shows receive coil voltage versus target distance, over a range of 100 cm.

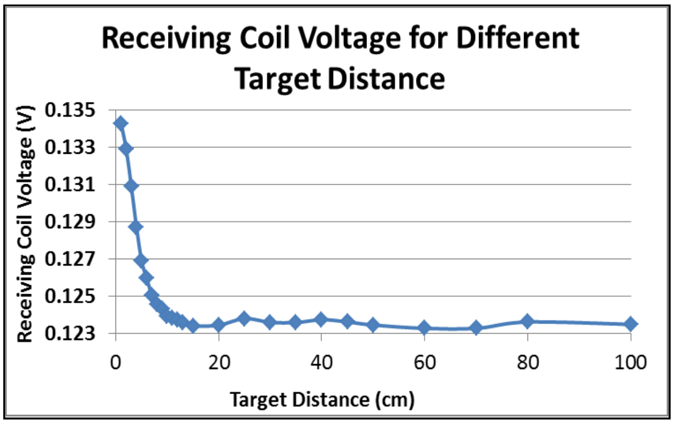

Figure 13: V_R vs target distance z for gold ring target

It can be seen that the metal detector output voltage responds to the target position for distances up to about 12 cm, and beyond this point there is little change in output voltage. This gives an indication of the maximum range of the detector under these conditions.

Figure 14 shows a similar curve to that in Figure 13, normalized to the no-target case (which is simulated by specifying the gold ring as “air”), and including the case where there are offsets of the receive and bucking coils, as in Scenario ‘A’.

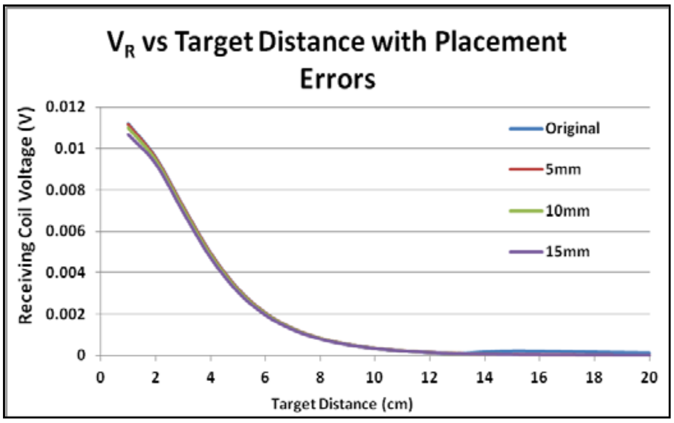

Figure 14: V_R vs target distance for 0 to 15 mm head offset

It can be seen that for these placement errors, there is apparently very little impact on the performance of the detector, with a maximum range of about 12 cm still possible. The receive coil voltage is slightly smaller for the larger errors, implying a poorer signal-to-noise ratio.

CONCLUSIONS

Performance of a VLF MD head was simulated using *JMAG*™, allowing for coil placement errors, and using receive coil leakage voltage as a performance measure. Two main scenarios were considered, in which the bucking coil remained concentric with either (A) the receive coil or (B) the transmit coil. It was found that for all displacements considered, MD performance declined with displacement. Errors could in principle be corrected by adjusting the bucking coil voltage. In scenario ‘B’ the corrections required were found to be much greater than in scenario ‘A’. The simulation was also able to show the performance of the detector with a gold ring target, and to predict its likely range.

REFERENCES

[1] E. S. Grosvenor and M. Wesson, "Alexander Graham Bell: The Life and Times of the Man Who Invented the Telephone," New York: Harry N. Abrams, Inc., 1997.

[2] M. Croll, "The History of Landmines," Great Britain: Leo Cooper, Pen & Sword Books Ltd, 1998.

[3] C. King, Ed. "Jane's Mines and Mine Clearance," London: Jane’s Information Group, 2005.

[4] S. Tumanski, "Induction coil sensors - a review," Meas. Sci. Technol. 18, pp. R31–R46, 2007.

[5] S. Yamazaki, H. Nakane, and A. Tanaka, "Basic Analysis of a Metal Detector," IEEE Trans. Instrumentation and Measurement, Vol. 51, No. 4, pp. 810-814, 2002.

[6] J.A. Corbyn, "Pulse induction metal detector," Wireless World, March 1980

[7] B. Candy, "Metal Detector Basics and Theory," Minelab Pty Ltd. Technical Report, 2007. Available online at: www.minelab.com/__files/f/11043/METAL%20DETECTOR%20BASICS%20AND%20THEORY.pdf (accessed: June 13, 2011)

[8] M. S. and M. I. Sharawi, "Design and Implementation of a Low Cost VLF Metal Detector with Metal-Type Discrimination Capabilities," Dubai: ICSPC 2007, pp. 480-483, ISBN: 978-1-4244-1235-8, 2007.

[9] Minelab Pty Ltd., http://www.minelab.com/asia/consumer, 2011

[10] F. H. Thompson, "Coil arrangement for search head of metal detector - has closed loop load coil between portions of transmit and cancel coils," US Patent US4255711-A, 1981.

[11] H-G. Doll, "Coil Assembly for Geophysical Prospecting," US Patent No. 2,807,777, September 1957.

[12] L.M. Nel, "Induction-based detection of vegetation-obscured tripwires," ME Thesis, Department of Electrical and Computer Engineering, The University of Auckland, New Zealand, 2009.

[13] L.J. Carter, "Landmines: Demining Practice," in The International Encyclopedia of Peace, N. Young, Ed., Oxford University Press, October 2009.

[14] L.J. Carter, S. Jayalath, and R. Edwin, "Developments in Electromagnetic Methods for Tripwire Detection," Proc. European Electromagnetics Conference (EUROEM 2008), Lausanne, July 2008.

[15] L.J. Carter and C.Y. Liao, "An optimal technology for detection of vegetation-obscured tripwires," Proc. SPIE: Detection and Remediation Technologies for Mines and Minelike Targets XI, Orlando [USA], April 2006.

[16] L.J. Carter and C.Y. Liao, "A new approach to detecting vegetation-obscured tripwires," Proc. First International Conference on Industrial and Information Systems (ICIIS 2006), Peradeniya [Sri Lanka], August 2006.

[17] C.Y. Liao, "Tripwire Detection Methods," ME Thesis, Department of Electrical and Computer Engineering, The University of Auckland, New Zealand, 2006.

[18] L.J. Carter and C.Y. Liao, "Sensing technologies for tripwire detection," First International Conference on Sensing Technology, Palmerston North, New Zealand, November 2005.